# Magnetotransport through antidot and dot lattices in two-dimensional structures

V. G. Burnett, A. L. Efros, and F. G. Pikus
*Department of Physics, University of Utah, Salt Lake City, Utah 84112*
(Received 27 April 1993)

The redistribution of electron density caused by magnetic gaps is explored for both dot and antidot lattices. It is assumed that the saddle points in the electron-density distribution determine the magnetotransport in these periodic systems. We show that the quantum Hall plateaus are shifted to lower magnetic fields in the case of antidot lattices and to higher magnetic fields in the case of dot lattices. Our theory is in a good quantitative agreement with the experimental data by Ensslin and Petroff for antidot systems. The results are obtained by computer simulation taking into account nonlinear screening by the electrons of two Landau levels. For one-level screening, we present an analytical solution of the nonlinear electrostatic problem.

## I. INTRODUCTION

Antidot or dot type lattices in two-dimensional structures can be created by electrostatic confinement using gate electrodes of special geometry,[1–4] holographically induced persistent photoconductivity,[5] focused ion-beam implantation,[6–8] or selective etching.[9,10] The transport properties of such lattices have been studied theoretically, using both classical[11–18] and quantum[19–22] approaches. Usually the confinement potential was considered in the one-electron approximation. Deruelle *et al.*[23] and Stern[24] have shown that electron screening decreases the confinement potential in an antidot lattice very effectively. In this paper we consider electron screening of the confinement potential in a strong magnetic field.

If the lattice period is much larger than all microscopic lengths, the confinement potential can be considered classically. In this case, the spatial distribution of electron density $n(\mathbf{r})$ can be found from the solution of the following electrostatic problem.[25,26] In regions with nonzero electron density (metallic regions) the electrochemical potential $\mu$ must be independent of $\mathbf{r}$. This condition takes the form

$$E_F(n) + F_c(\mathbf{r}) + \frac{e^2}{\kappa}\int \frac{n(\mathbf{r}')d^2r'}{|\mathbf{r}-\mathbf{r}'|} = \mu. \qquad (1)$$

Here $E_F(n)$ is the local chemical potential, which is a function of the local density $n(\mathbf{r})$, $F_c(\mathbf{r})$ is the electrostatic confinement potential energy, and $\kappa$ is the dielectric constant. The third term is the electrostatic potential energy, created by the two-dimensional electron gas (2DEG). In regions with zero electron density (dielectric regions), the total potential energy of an electron

$$F(\mathbf{r}) = F_c(\mathbf{r}) + \frac{e^2}{\kappa}\int \frac{n(\mathbf{r}')d^2r'}{|\mathbf{r}-\mathbf{r}'|} \qquad (2)$$

must be larger than the electrochemical potential $\mu$ in the metallic regions. The solution of this nonlinear problem includes finding the boundaries between metallic and dielectric regions.

Throughout this problem only the local chemical potential contains information about the density of states and other microscopic properties of the system. It is defined as $E_F = dH/dn$, where $H$ is the energy density of the *homogeneous* electron liquid on a positive background. At high electron density, without a magnetic field, $E_F(n)$ is close to the Fermi energy of a free electron gas, but at low density it is determined by correlation and can be negative.[25]

The spatial variation of the first term in Eq. (1) is of the order of $e^2n'/\kappa q_s$, where $n'$ is the local variation in electron density and $q_s = (2\pi e^2/\kappa)dn/dE_F$ is the reciprocal screening radius. The third term is of the order of $e^2n'P/\kappa$, where $P$ is the characteristic size of the confinement potential, say, a period of an antidot lattice. If $Pq_s >> 1$, one can neglect the first term and obtain an electrostatic problem which does not require any information about the microscopic properties of the system. This approximation assumes that the total electrostatic potential is constant in metallic regions, which means "perfect" screening. This perfect screening approximation has been used for calculations of the density distribution in an antidot lattice,[23] in a random potential,[27] and for some one-dimensional problems.[28,29]

The aim of this paper is to take into account the effect of gaps in the chemical potential, caused by a strong magnetic field, on the electron distribution. These gaps appear in the problem as discontinuities of the local chemical potential $E_F(n)$ in Eq. (1). In this paper we study only the two-level screening problem, when there is one discontinuity of $E_F(n)$ in the range of electron densities under consideration. In this situation, only particles in the higher Landau level (LL) and holes in the lower LL are responsible for the screening. Thus, we have metallic regions of particle or hole types, and dielectric regions with neither particles nor holes. The electron gas in the dielectric regions has a quantized density, is incompressible, and cannot screen the external potential.

Suppose that without a magnetic field the electron density of an inhomogeneous system varies in the interval $n_{\min} \le n(\mathbf{r}) \le n_{\max}$. If the magnetic field is so strong that $n_0 = eB/2\pi\hbar c > n_{\max}$, it does not affect the elec-

 

tron distribution at all. Actually, the perfect screening approximation is valid in a magnetic field if the chemical potential $E_F(n)$ has no singularities at all electron densities.[25,30] The only specifics of this case is that all electrons are in the lowest LL and that they have a negative screening radius $q_s^{-1}$. The magnitude of $q_s$ is of the order of $n^{-1/2}$, and in a smooth confinement potential the variation of the first term in Eq. (1) can still be neglected. Thus, the distribution of an electron density in a strong magnetic field is the same as without a magnetic field.

Assume now that $n_0 < n_{\max}$. Then in all points, where the density $n(\mathbf{r})$ without a magnetic field is greater than $n_0$, electrons either occupy the next LL or move to regions with lower electron density. To occupy the next level, they must overcome a gap. Thus, at small values of $n_{\max} - n_0$ the second way is preferable: electrons are pushed out of the regions with high density, so that $n_0$ becomes the maximum density in the system. Figure 1 demonstrates this behavior for the case of a dot. However, now the confinement potential is not completely compensated by electron screening. The resulting electrostatic potential attracts electrons to the regions where the electrons have been pushed out of. This potential increases with $n_{\max} - n_0$. When it becomes larger than the gap in the chemical potential, electrons occupy the next LL in the regions where the density was highest without a magnetic field. These regions are surrounded by strips, where the density is exactly equal to $n_0$, and the potential is not large enough to overcome the gap. With decreasing magnetic field these strips move toward low density regions [Figs. 1(c) and 1(d)]. The spatial width of a strip has been estimated by Efros[31] for the case of a smooth random potential in the approximation of a small gap. Chklovskii, Shklovskii, and Glasman[28] found an exact expression for this width in the same approximation for a one-dimensional smooth potential.

In this paper we find the redistribution of the electron density caused by a magnetic field, in a periodic confinement potential. These results are applied to magnetotransport in antidot and dot lattices with large periods. We explore an idea that the plateaus of the quantum Hall effect in a periodic system occur when saddle points in the electron-density distribution are occupied by the incompressible phase of the liquid.[23,25] For a periodic system with a square lattice, the saddle points are in the middle of the line connecting neighboring dots or antidots. Thus, the interval of magnetic field corresponding to a plateau can be found from the condition that the density in the saddle point is equal to $Mn_0$, where $M$ is

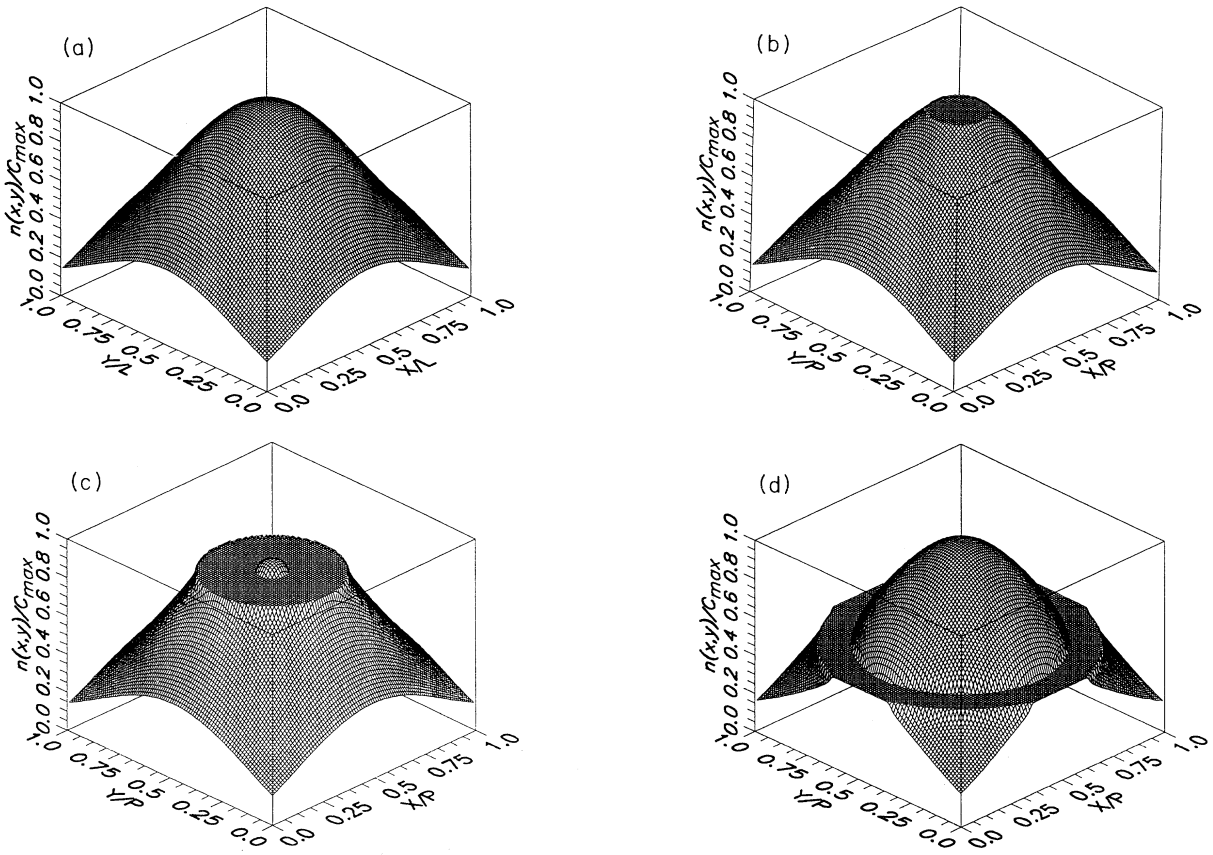


FIG. 1. The electron charge density in a unit cell of a dot lattice. The external charge density is given by Eq. (4) with $P = 5000$ Å. (a) High magnetic field, $n_0 > n_{\max}$, screening is complete. (b) $n_0/C_{\max} = 0.96$, electrons are pushed from the central dielectric region, where $n(\mathbf{r}) = n_0$, to the regions with lower density. (c) $n_0/C_{\max} = 0.83$, the appearance of the electrons at the higher LL. (d) $n_0/C_{\max} = 0.47$, the dielectric region occupies the saddle point.

an integer. Using this idea we show that the plateaus in $\rho_{xy}$ for the antidot-type lattice are mostly above the line $\rho_{xy}^{(0)} = B/en_s^{(0)}c$, where $n_s^{(0)}$ is the density in the saddle point without a magnetic field. This is confirmed very nicely by the experimental data of Ensslin and Petroff.[32] For the dot-type lattice plateaus should be located below this line.

## II. ANALYTICAL SOLUTION FOR A SINGLE DOT

The analytical solution for a single dot in a magnetic field is very instructive for understanding the redistribution of electron charge in a magnetic field. Such a solution can be obtained for the case of an electron distribution with axial symmetry and only one incompressible region, using the method proposed in Ref. 23. The total charge density of the dot is

$$\sigma(\mathbf{r}) = e\left[\Sigma(\mathbf{r}) + \bar{n} - n(\mathbf{r})\right], \tag{3}$$

where $\Sigma(\mathbf{r})$ is an external charge density, $\bar{n}$ stands for the positive background density, which is equal to the average electron density, and $n(\mathbf{r})$ is the local electron density. We choose the external density in the form of a Gaussian function with two parameters, $C_{\max}$ and $L$:

$$\Sigma(\mathbf{r}) = C_{\max} e^{-\frac{r^2}{L^2}}. \tag{4}$$

Actually, such a solution can be obtained for any function $\Sigma(\mathbf{r})$ with axial symmetry.

The charge density $\sigma(\mathbf{r})$ must tend to zero at $r \to \infty$. Thus, $\lim_{r\to\infty} n(\mathbf{r}) = \bar{n}$. Without an applied magnetic field, in the perfect screening approximation $\sigma(\mathbf{r}) = 0$ everywhere. Then $n(\mathbf{r}) = \Sigma(\mathbf{r}) + \bar{n}$. It also follows that the maximum electron density is $n_{\max} = C_{\max} + \bar{n}$. For a large magnetic field, when $n_0 > n_{\max}$, the electron distribution will be the same as it was without a magnetic field, i.e., the external charge of the dot will be completely screened. But at lower $B$, when $\bar{n} < n_0 < n_{\max}$, the electron density $n(\mathbf{r})$ is altered from that of perfect screening. The 2DEG in this case will consist of a circular dielectric region of radius $r_d$ and density $n_0$ and a metallic region with density $n(\mathbf{r}) < n_0$ that extends over the rest of the 2DEG. We choose the electrostatic potential $\phi(\mathbf{r})$ for this problem to be zero at infinite distance from the center of the dot. Then $\mu = 0$.

The solution of this electrostatic problem can be found from the equations[23]

$$\sigma(r) = 2\kappa \int_0^{r_d} \frac{dt}{\sqrt{r^2 - t^2}} \frac{df}{dt}, \qquad r > r_d, \tag{5}$$

$$f(t) = \frac{4}{\kappa} \int_0^t \frac{r\sigma(r)dr}{\sqrt{t^2 - r^2}}, \qquad t < r_d. \tag{6}$$

Substituting Eqs. (3) and (4) into Eq. (6) and taking into account that $n(\mathbf{r}) = n_0$ for $r < r_d$, we obtain

$$f(t) = \frac{4e}{\kappa}\left\{ C_{\max} \int_0^t \frac{re^{-\frac{r^2}{L^2}}dr}{\sqrt{t^2 - r^2}} + (\bar{n} - n_0) \int_0^t \frac{rdr}{\sqrt{t^2 - r^2}} \right\}, \quad t < r_d. \tag{7}$$

The integral in the first term of Eq. (7) can be expressed through the Dawson function:

$$\frac{1}{L}\int_0^t \frac{re^{-\frac{r^2}{L^2}}dr}{\sqrt{t^2 - r^2}} = e^{-t^2/L^2} \int_0^{t/L} e^{u^2} dx \equiv \mathrm{Daws}\left(\tfrac{t}{L}\right). \tag{8}$$

Thus,

$$f(t) = -\frac{4e}{\kappa}\left\{(n_0 - \bar{n})t + C_{\max}\mathrm{Daws}\left(\tfrac{t}{L}\right)\right\}, \quad t < r_d. \tag{9}$$

The derivative $df/dt$ can be found from Eq. (9):

$$\frac{df}{dt} = -\frac{4e}{\kappa}\left\{(n_0 - \bar{n}) + C_{\max}\left[1 - 2\frac{t}{L}\mathrm{Daws}\left(\frac{t}{L}\right)\right]\right\}. \tag{10}$$

Substituting this expression into Eq. (5) we can write the final result for the charge density:

$$\sigma(r) = \frac{2eC_{\max}}{\pi}\left[\left(1 - \frac{n_0 - \bar{n}}{C_{\max}}\right)\arcsin\left(\frac{r_d}{r}\right) - 2\int_0^{\frac{r_d}{L}} \frac{x\mathrm{Daws}\,(x)}{\sqrt{\frac{r^2}{L^2} - x^2}}dx\right], \quad r > r_d. \tag{11}$$

Using Eqs. (5) and (10), one can show that it has a singularity at $r = r_d$:

$$\sigma(r) - \sigma(r_d) = \frac{2\sqrt{2}eC_{\max}}{\pi}\left\{1 - \frac{n_0 - \bar{n}}{C_{\max}}\left[1 + 2\left(\frac{r_d}{L}\right)^2\right]\right\} \times\sqrt{\frac{r}{r_d} - 1}, \quad r - r_d \ll r_d. \tag{12}$$

The dependence of $r_d$ upon $n_0$ is determined from the condition[23] $f(r_d) = 0$, which takes the form

$$\frac{n_0 - \bar{n}}{C_{\max}} = \frac{\mathrm{Daws}(r_d/L)}{r_d/L}. \tag{13}$$

The electron density $n(\mathbf{r})$ can be found now from Eqs. (3)–(5), (13), and (11). Figure 2(a) shows the dependence of $n(L)/C_{\max}$ on $n_0/C_{\max}$. To compare the analytical solutions with the results of our computer modeling of a dot lattice (see Sec. IV A), we put $\bar{n} = 0$. For high magnetic fields, when $n_0 > C_{\max}$, the electron density $n(\mathbf{r})$ is independent of magnetic field and equal to $\Sigma(\mathbf{r})$. Thus, $n(L)/C_{\max} = e^{-1}$ at $n_0/C_{\max} \geq 1$. The density $n(L)$ increases with decreasing magnetic field due to the push-out of electrons from the central region of the dot. Eventually, as $n_0$ is lowered, $n(L)$ becomes equal to $n_0$, and remains equal to $n_0$ at lower magnetic fields. Figure 2(b) shows the local resistivity $\rho_{xy}(\mathbf{r}) = (h/e^2)n_0/n(\mathbf{r})$. At small magnetic fields, it has an integer plateau, and then it increases with magnetic field; this increase becomes linear at $n_0/C_{\max} > 1$. This

analytical theory cannot describe the appearance of electrons in the next LL at the center of a dot [see Fig. 1(c)]. However, it can predict the value of the magnetic field when this first occurs. It happens when the electrostatic potential $\phi(\mathbf{r})$ at the center of the dot becomes equal to $\Delta/|e|$, where $\Delta$ is the distance between the LL's. This potential is given by the equation

$$\phi(0) = \int_0^{r_d} \frac{f(t)}{t} dt. \tag{14}$$

Figure 3 shows $\phi(0)\kappa/eLC_{\max}$ as a function of $n_0/C_{\max}$. The critical magnetic field, at which one-level screening fails, can be found from this plot. The screening by two LL's will eventually give way to three-level screening and so on as the magnetic field is decreased.

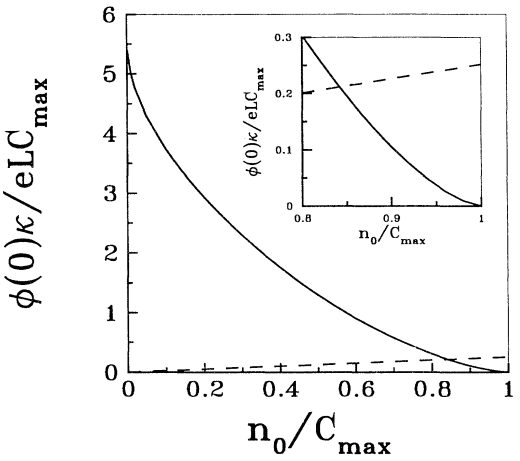


FIG. 3. Electrostatic potential in the center of a single dot in units of $eLC_{\max}/\kappa$, as obtained by analytical theory, is plotted against $n_0/C_{\max}$ (solid line). The average density $\bar{n} = 0$. The dashed line shows $\Delta/|e|$ in the same units on $n_0/C_{\max}$. For even filling factors, $\Delta = 2\pi\hbar^2 n_0/m$. The material parameters used are for GaAs, $L = 2500$ Å. The intersection of solid and dashed lines, which corresponds to $|e|\phi(0) = \Delta$, determines the value of magnetic field, when the electrons first appear at the higher LL. The inset magnifies the intersection area.

## III. MODELING DOTS AND ANTIDOTS

### A. Equations for nonlinear screening by two Landau levels

In this paper, it is assumed that only electrons in the two highest occupied LL's participate in screening. This approximation is valid for large enough magnetic field.

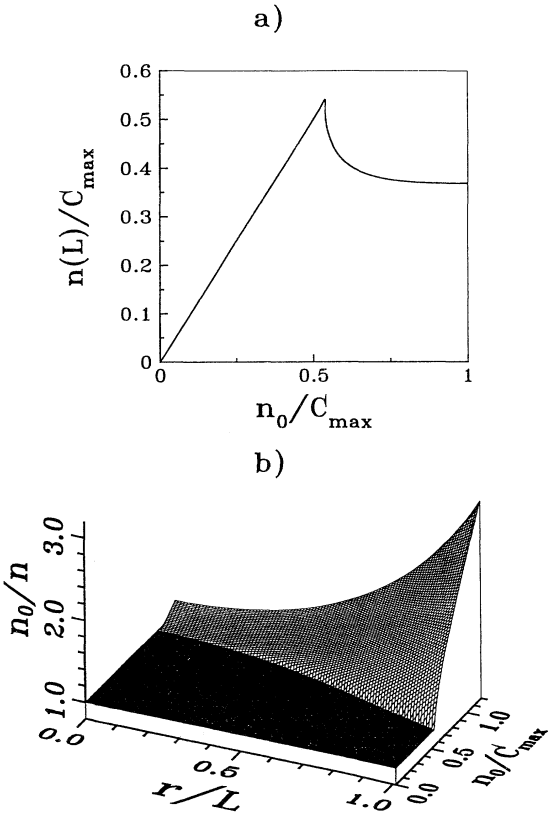


FIG. 2. Results of analytical theory for a single dot. (a) electron density $n(L)$ as a function of $n_0/C_{\max}$. (b) Local Hall resistivity $\rho_{xy}(\mathbf{r}) = (h/e^2)n_0/n(\mathbf{r})$ as a function of $\mathbf{r}/L$ and $n_0/C_{\max}$. The average density $\bar{n} = 0$.

For two-level screening, there are two types of metallic regions: hole and particle. In the hole regions the higher LL is completely empty; we describe the charge in these regions by the density of unoccupied states $n_h(\mathbf{r})$ in the lower LL, called the hole density. In the particle regions, the higher LL is partially occupied, while the lower one is completely occupied; the charge in these regions is characterized by the density of electrons in the second LL, $n_p(\mathbf{r})$. The density of electron charge $n(\mathbf{r})$ is defined as

$$n(\mathbf{r}) = n_p(\mathbf{r}) - n_h(\mathbf{r}). \tag{15}$$

The average value of $n(\mathbf{r})$ is zero at a filling factor $M$, where $M$ is the number of lower LL's under consideration. Thus, the reference point for $n(\mathbf{r})$ is $Mn_0$.

Now one can use Eq. (1), taking into account the singularity in the function $E_F(n)$:

$$E_F(+0) - E_F(-0) = \Delta. \tag{16}$$

For the integer quantum Hall effect, $\Delta$ is the LL separation. This singularity produces dielectric strips, where $n(\mathbf{r}) = 0$. These strips separate the metallic regions of different types.

One can find the boundaries of all the regions from the conditions

$$\begin{aligned} F(\mathbf{r}) &= \mu \quad \text{if } n(\mathbf{r}) > 0, \\ F(\mathbf{r}) &= \mu + \Delta \quad \text{if } n(\mathbf{r}) < 0, \\ \mu < F(\mathbf{r}) &< \mu + \Delta \quad \text{if } n(\mathbf{r}) = 0. \end{aligned} \tag{17}$$

Here $F(\mathbf{r})$ is the potential energy of an electron in the higher LL. These equations were derived with the assumption that $n_e(\mathbf{r})$, $n_h(\mathbf{r}) \leq n_0$ at all $\mathbf{r}$.

### B. Computer program

A solution of the above electrostatic problem cannot be obtained analytically for a periodic arrangement of dots (or antidots), even for the case of no magnetic field. We have solved this problem by performing a computer modeling. In our model we actually calculate the electron distribution within one square unit cell, and the periodic array was simulated by using the quasiperiodic boundary conditions (for details see Ref. 27). The side of the square is equal to the period of the system $P$. The continuous charge distribution was approximated by point charges on the sites of a square lattice. This approximation is valid if variations in the charge distribution and the potential occur over distances much larger than the lattice constant.

Our computer program first generates the external charge on the lattice, and then calculates the resulting potential at each point. After this, the program goes through each lattice point, and compares the total potential, created by both the external and the electron charges, with the chemical potential $\mu$. If the potential at a point is greater than $\mu$ and $n_p$ is nonzero, a small particle charge is removed from the lattice point, but if the potential is below $\mu$, charge is added. At the same time, if the potential at the lattice point is greater than $\mu + \Delta$, a small hole charge is added to the lattice point, and if the potential is less than $\mu + \Delta$ and the hole charge $n_h$ is nonzero, a portion of the hole charge is removed. Every time we change a charge of a lattice site by some amount, we also change the background charge density in such a way that the neutrality of the whole system is maintained in each step. These iterations continue until the conditions (17) are satisfied everywhere within a given accuracy.

The algorithm, described above, allows one to find the electron charge distribution for given values of $\mu$ and $\Delta$. However, one must use some additional criteria to choose the chemical potential for each magnetic field. We have assumed that the total electron density in the system is independent of magnetic field, and, therefore, is always equal to the average electron density $N$ without a magnetic field:

$$Mn_0 + \bar{n}(\mu) = N, \tag{18}$$

where $\bar{n}(\mu)$ is an average electron density $n(\mathbf{r})$ for a given value of $\mu$. The condition (18) defines $\mu$ as a function of $\Delta$. Note that $\Delta$ is also related to $n_0$. For the gaps with even filling factors $n_0 = m\Delta/2\pi\hbar^2$, where $m$ is an electron mass.

In our computer modeling of a dot lattice the external charge density inside a unit cell has the form of Eq. (4), where $L$ equals the half period of the dot lattice $P$. The average electron density $N$ was chosen to be equal to the average external charge density, so that the whole system is always neutral.

For an antidot lattice, we use the model proposed in Ref. 23. In this model, the external charge distribution within a unit cell of the lattice of antidots is assumed to be a disk of a radius $a$ and constant charge density $\Sigma$, where $\Sigma$ is much larger than the average electron density $N$. Without a magnetic field, this large charge repels the electrons of the 2DEG and forms a depletion region with zero electron density in the center of each antidot. In a strong magnetic field, the electron distribution will be the same as it was without a magnetic field, and all electrons will belong to the lowest LL. The depletion region exists also at lower magnetic field, when the electrons of the two LL's participate in the screening. In this situation one can still use the conditions (17), but the hole density $n_h$ must not exceed $n_0$. The program described above can be easily modified to include this restriction.

## IV. RESULTS OF COMPUTER MODELING

### A. Dots in a magnetic field: Results of modeling and comparison with analytical theory

Our results for the density distribution in a periodic array of dots are shown in Fig. 1 at different magnetic fields. These results are discussed qualitatively in the Introduction. Using the analytical theory (see Sec. II), we can find the magnetic field when electrons first appear in the higher LL. This occurs when the electrostatic potential in the center of the dot $\phi(0)$ becomes equal to $\Delta/|e|$. The way to find the corresponding $n_0/C_{\max}$ is shown in Fig. 3. For a dot lattice period 5000 Å this gives $n_0/C_{\max} = 0.84$, while computer modeling gives $n_0/C_{\max} = 0.83$.

It has been proposed in Ref. 23 that the plateaus of the Hall resistivity $\rho_{xy}$ in a periodic system occur when the incompressible liquid occupies saddle points of the electron-density distribution. Chklovskii, Matveev, and Shklovskii[29] and Ruzin[33] have argued that the density in the saddle points $n_s$ determines $\rho_{xy}$ even between plateaus, namely

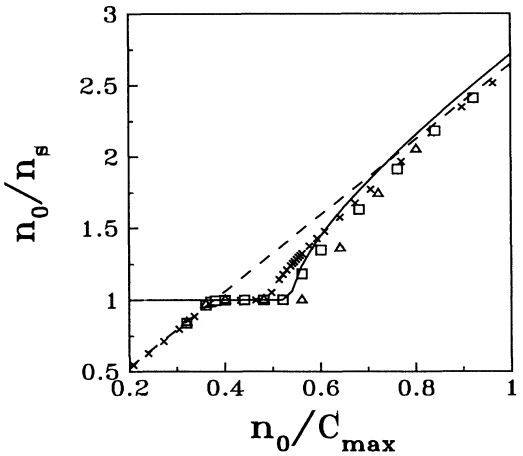


FIG. 4. Hall resistivity $\rho_{xy}$ vs $n_0/C_{\max}$ for a dot lattice for different periods: $P = 5000$ Å for crosses, $P = 2500$ Å for squares, $P = 500$ Å for triangles. The solid line shows the analytical result for a single dot. The dashed line is the classical Hall resistance $\rho_{xy}^{(0)}$.

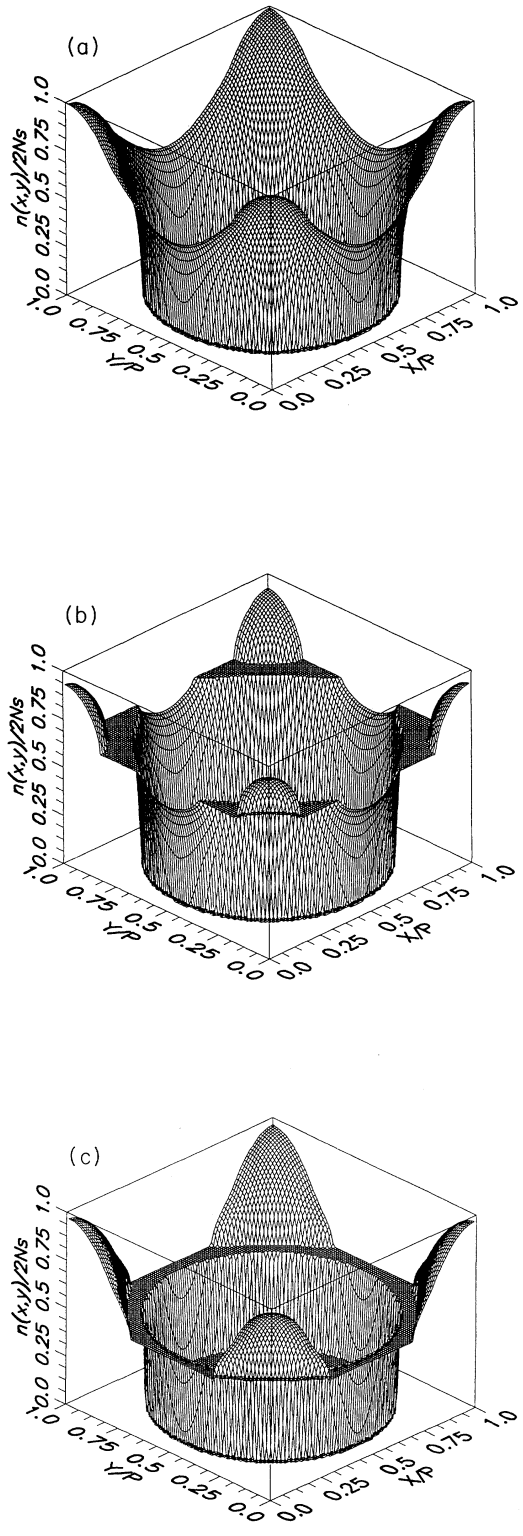


FIG. 5. The electron density in a unit cell of an antidot lattice. The external charge density $\Sigma = 4 \times 10^{12}$ cm$^{-2}$ is uniform within a disk of radius $a = 40$ nm in the center of the antidot. The lattice period $P = 200$ nm. (a) High magnetic field, $n_0 > n_{\max}$, screening is complete. (b) $n_0/\sigma = 0.077$, the dielectric strip, separating two metallic regions, is formed. (c) $n_0/\Sigma = 0.058$, the dielectric region occupies the saddle point.

$$\rho_{xy} = \frac{h}{e^2}\frac{n_0}{n_s}. \tag{19}$$

We use Eq. (19) to find the Hall resistivity from the saddle point density $n_s$, which is calculated by our program. In our arrays of dots and antidots the saddle points are in the middle of the lines connecting neighboring dots (or antidots).

Our results are shown in Fig. 4, where the $\rho_{xy}$ is plotted against $n_0/C_{\max}$, for three lattice periods. The dashed line shows $\rho_{xy}^{(0)} = (h/e^2)n_0/n_s^{(0)}$, where $n_s^{(0)}$ is the saddle point density without a magnetic field. Thus, this line corresponds to the classical Hall effect in a strong magnetic field. The most important feature of our results is that all points, obtained by computer simulation, are below this classical line. This effect is discussed in the next subsection.

The solid line shows the result of our analytical theory of one-level screening in a single dot (see Sec. II).

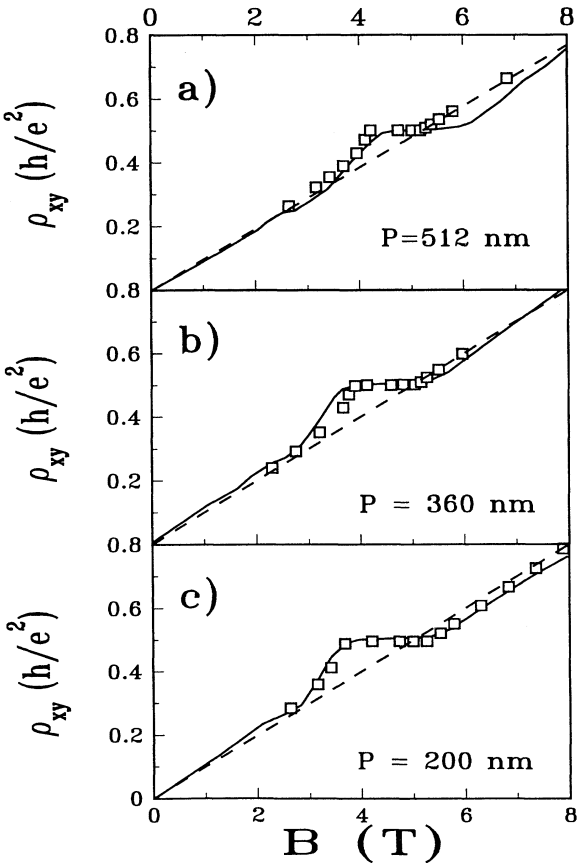


FIG. 6. Hall resistivity $\rho_{xy}$ as a function of magnetic field for antidot lattice. The experimental results by Ensslin and Petroff (Ref. 32) are shown by the solid lines. Squares are the results of our calculations. Dashed lines show the classical Hall resistivity $\rho_{xy}^{(0)} = (h/e^2)n_0/n_s^{(0)}$. (a) $L = 512$ nm, $n_s^{(0)} = 2.5 \times 10^{11}$ cm$^{-2}$, $\Sigma = 1.15 \times 10^{13}$ cm$^{-2}$, $a = 40$ nm; (b) $L = 360$ nm, $n_s^{(0)} = 2.4 \times 10^{11}$ cm$^{-2}$, $\Sigma = 9.6 \times 10^{12}$ cm$^{-2}$, $a = 40$ nm; (a) $L = 200$ nm, $n_s^{(0)} = 2.4 \times 10^{11}$ cm$^{-2}$, $\Sigma = 4.0 \times 10^{12}$ cm$^{-2}$, $a = 40$ nm.

To adjust this result to a periodic array of dots, we put $\bar{n} = 0$ and $L = P/2$ in Eqs. (7)–(11) and calculate $n(L)$ as a function of a magnetic field. The analytical theory corresponds to an infinite $\Delta$, so it does not describe the low-field ending of the plateau. However, it gives a reasonable description of the high-field part of the curve. It can be seen from Eqs. (13) and (11) that the analytical result for $n(L)$ is independent of $L$, while the results of the computer simulation show that the plateau width increases as $P$ decreases. This discrepancy occurs because the analytical theory does not take into account two effects which shift the high-field end of the plateau in opposite directions. First, in the analytical calculations we consider only one dot, while in a dot lattice the electrons are pushed into the saddle point by two neighboring dots. The second effect is that the analytical theory assumes that the dielectric region forms a disk inside the dot. In the simulation, the dielectric region becomes a narrow ring before the quantized density reaches the saddle point.

### B. Antidots in a magnetic field: Results of modeling and comparison with experiment

In modeling an antidot lattice we choose the parameters to fit the experimental data by Ensslin and Petroff.[32] The values of the external charge density $\Sigma$ were taken from Ref. 23. The average electron density $N$ has been found from the condition that the saddle point density $n_s$ without a magnetic field coincides with the density obtained by Shubnikov–de Haas measurements.

Figure 5 shows the electron-density distribution in a unit cell of the antidot lattice. The distribution without a magnetic field or in a very large magnetic field, when all electrons are in the lowest LL, is shown in Fig. 5(a). Figure 5(b) demonstrates the appearance of the quantized density with decreasing magnetic field. The situation when the saddle point density becomes quantized is illustrated in Fig. 5(c).

Figure 6 shows $\rho_{xy}$ as obtained from data by Ensslin and Petroff for periods of 200 nm and 300 nm. The dashed line shows the classical Hall resistivity $\rho_{xy}^{(0)} = (h/e^2)n_0/n_s^{(0)}$, where $n_s^{(0)}$ is the saddle point density without magnetic field. Contrary to the case of the dot lattice (see Fig. 4), the plateau is shifted toward lower magnetic field with respect to the classical line both in our calculations and in experimental data for the small periods.

The shift of the plateaus in the opposite directions for dot and antidot lattices can be explained qualitatively in terms of the electron density distribution near the saddle point without a magnetic field. One can see from Figs. 1 and 5 that the two curvatures of the density distribution at the saddle point are very different. The curvature along the line connecting two neighboring dots or antidots is much greater than the curvature in the perpendicular direction. Then, in the first approximation, we can consider the vicinity of the saddle point in the dot lattice as a long parabolic trough with its axis perpendicular to the line, connecting neighboring dots. The minimum electron density without a magnetic field is equal to $n_s^{(0)}$. The magnetic field always depletes the regions with $n(\mathbf{r}) > n_0$ and enhances the density in the regions with $n(\mathbf{r}) < n_0$ [see Figs. 1(c), 1(d), 5(b), and 5(c)]. In our approximation the density at the bottom of the trough is the lowest density in the system. If $n_0 < n_s^{(0)}$ and $2n_0 > C_{\max}$, the chemical potential $E_F(n)$ has no singularities for all values of $n(\mathbf{r})$ in the dot lattice. Then we have perfect screening and the density at the bottom of the trough is independent of magnetic field and equals $n_s^{(0)}$. With increasing magnetic field the density at the bottom becomes equal to $n_0$ only when $n_0$ reaches $n_s^{(0)}$. Therefore, the low-field end of the plateau of $\rho_{xy}$ is exactly on the classical line $\rho_{xy}^{(0)} = (h/e^2)n_0/n_s^{(0)}$, and all the plateau is below this line (see Fig. 4).[34]

For the case of the antidot lattice, the vicinity of the saddle point can be approximated as an inverse parabolic trough with maximum density $n_s^{(0)}$. The same consideration shows that in this case the plateau must be above the classical line.

The trough approximation is valid in the limit of a very large ratio of the curvatures in a saddle point. At a finite ratio, the plateaus are just shifted with respect to the classical line.

One can see from Fig. 6 that our results are in good quantitative agreement with the experimental data of Ref. 32 for the lattice periods 200 and 360 nm. For the 512 nm period the classical line crosses the experimental plateau nearly in the center, while our simulation gives a large shift. We think that at such large periods all curvatures of the regular density distribution are small, and that they are strongly affected by random fluctuations. Then the situation becomes more or less the same as in homogeneous disordered systems, where the plateaus are usually not shifted with respect to the classical line.

Finally, we considered the redistribution of electron density, caused by a magnetic field, for periodic systems of dots and antidots. We show that this redistribution results in a shift of the plateau of the integer quantum Hall effect in different directions for dots and antidots. Our results are in good agreement with the experimental data of Ensslin and Petroff.[32]

## ACKNOWLEDGMENTS

We are grateful to H. Kroemer and P. M. Petroff for the stimulating discussions. This work was supported by the Center for Quantized Electronic Structures (QUEST) of UCSB under subagreement KK3017. We acknowledge support from the San Diego Supercomputer Center, where the computations have been performed.

[1] W. Winkler, J. P. Kotthaus, and K. Ploog, Phys. Rev. Lett. **62**, 1177 (1989).
[2] A. Lorke, J. P. Kotthaus, and K. Ploog, Superlatt. Microstruct. **9**, 103 (1991); Phys. Rev. B **44**, 3447 (1991).
[3] R. Schuster, K. Ensslin, J. P. Kotthaus, M. Holland, and C. Stanley, Phys. Rev. B **47**, 6843 (1992).
[4] J. Weis, R. J. Haug, K. v. Klitzing, and K. Ploog, Phys. Rev. B **46**, 12 837 (1992).
[5] R. R. Gerhards, D. Weiss, and K. v. Klitzing, Phys. Rev. Lett. **62**, 1173 (1989).
[6] P. M. Petroff *et al.*, J. Vac. Sci. Technol. B **9**, 3074 (1991).
[7] K. Ensslin and P. M. Petroff, Phys. Rev. B **41**, 12 307 (1990).
[8] G. M. Sundaram *et al.*, Phys. Rev. B **47**, 7348 (1993).
[9] J. N. Randall, M. A. Reed, T. M. Moore, R. J. Matyi, and J. W. Lee, J. Vac. Sci. Technol. B **6**, 302 (1988).
[10] K. Y. Lee *et al.*, J. Vac. Sci. Technol. B **8**, 1366 (1990).
[11] T. Geisel, A. Zacherl, and G. Radons, Phys. Rev. Lett. **59**, 2503 (1987).
[12] T. Geisel, R. Ketzmerick, and G. Petschel, Phys. Rev. Lett. **66**, 1651 (1991); **67**, 3536 (1991).
[13] J. Wagenhuber, T. Geisel, P. Niebauer, and G. Obermair, Phys. Rev. B **45**, 4372 (1992).
[14] G. Kirczenof, Phys. Rev. B **46**, 1439 (1992).
[15] J. U. Nockel, Phys. Rev. B **46**, 15 348 (1992).
[16] R. Fleischmann, T. Geisel, and R. Ketzmerick, Phys. Rev. Lett. **68**, 1367 (1992).
[17] E. M. Baskin, G. M. Gusev, Z. D. Kvon, A. G. Pogosov, and M. V. Entin, Pis'ma Zh. Eksp. Teor. Fiz. **55**, 649 (1992) [JETP Lett. **55**, 678 (1992)].
[18] G. Gumbs and D. Huang, Phys. Rev. B **46**, 12 822 (1992).
[19] P. G. Harper, Proc. R. Soc. London Ser. A **68**, 874 (1955).
[20] M. Ya. Azbel', Zh. Eksp. Teor. Fiz. **46**, 929 (1964) [Sov. Phys. JETP **19**, 634 (1964)].
[21] D. R. Hofstadter, Phys. Rev. B **14**, 2239 (1976).
[22] Y. Takagaki and D. K. Ferry, Phys. Rev. B **45**, 8506 (1992).
[23] T. Deruelle, K. Ensslin, P. M. Petroff, A. L. Efros, and F. G. Pikus, Phys. Rev. B **45**, 9082 (1992).
[24] F. Stern, Bull. Am. Phys. Soc. **38**, 54 (1993).
[25] A. L. Efros, Solid State Commun. **65**, 1281 (1988).
[26] C. W. J. Beenakker, Phys. Rev. Lett. **64**, 216 (1990).
[27] A. L. Efros, F. G. Pikus, and V. G. Burnett, Phys. Rev. B **47**, 2233 (1993).
[28] D. B. Chklovskii, B. I. Shklovskii, and L. I. Glasman, Phys. Rev. B **46**, 4026 (1992).
[29] D. B. Chklovskii, K. A. Matveev, and B. J. Shklovskii, Phys. Rev. B **47**, 12 605 (1993).
[30] A. L. Efros, Solid State Commun. **67**, 1019 (1988).
[31] A. L. Efros, Phys. Rev. B **45**, 11 354 (1992).
[32] K. Ensslin and P. M. Petroff, Phys. Rev. B **41**, 12 307 (1990).
[33] I. M. Ruzin, Phys. Rev. B **47**, 15 727 (1993).
[34] The same effect can be observed in the two-terminal conductance of a narrow channel (Ref. 29).